1. INTRODUCTION

In the later half of nineteenth century, the steel was used in a big way in the construction industry. As the steel member was thin and slender, stability became an important design consideration. With the introduction of composite materials, the research in stability analysis of beams, plates and shells has grown exponentially. Steel and composite structural elements (beams, plates and shell panels) used in aircrafts, spacecrafts, ships, bridges and offshore structures are subjected to a variety of static and dynamic loads during their life span and may undergo static and dynamic instabilities. The structural instability may lead to large deflections or large amplitude vibrations of the structural elements leading to global or local failures. Hence, buckling instability characteristics have become important design considerations.

Often, plates are a part of complex structural system and hence load coming on it may not be always uniform. For example, in the case of I-beam or wide flanged beam subjected to bending moment at the ends or lateral loads on the flange, the web of the beam is subjected to non-uniform inplane loads. The load exerted on the aircraft wings, or on the stiffened plate in the ship structures or on the slabs of a multi-storey building by the adjoining structures usually is non-uniform. The type of distribu-tion in an actual structure depends on the relative stiffnesses of the adjoining elements. Behaviour of structures subjected to non- uniform inplane compressive loading and shear loading is important in aircraft, civil and ship-building industries. Much work has been reported in the literature on the buckling of rectangular plates subjected to uniform inplane loading. However, very few papers deal with the buckling of plates subjected to non-uniform inplane loads. Buckling of plates subjected to and parabolic inplane compressive loading was obtained by earlier researchers based on unrealistic inplane stress distribution.

The development of the governing partial differential equation defining small lateral deflections of the middle surface of thin plates, as well as the development of the companion relationships, is based on certain assumptions adopted because of prior knowledge about the behavior of beams. Because of the limitation of small deflections,

1. The middle surface is assumed to remain unstrained. Because of the limitation of thinness,

2. Normals to the middle surface before deformation remain normal after deformation, and
3. Normal stresses in the direction transverse to the plate are neglected.
4. The material is homogeneous, isotropic, continuous, and linearly elastic.

The most commonly encountered problem in stability is the bifurcation buckling in which the perfect structure looses its stability by switching from one equilibrium state to another equilibrium state. The load associated with the bifurcation point is known as the critical buckling load. Bifurcation point is defined as the point where a perfect structure switches from an equilibrium path (primary path) to another equilibrium path i.e. secondary path. Characterisation of perfect structure can be done by bifurcation point and imperfect structure by limit point. Limit point is the point on equilibrium path, which corresponds to zero structural stiffness. Two types of buckling exist in the perfect elastic structures: bifurcation buckling and nonlinear collapse. Nonlinear analysis is used to predict the nonlinear collapse. Snap-through and snap-back buckling is the phenomenon of nonlinear structural analysis.
When a slender structure is loaded in compression, for small loads it deforms with hardly any noticeable change in geometry and load carrying ability. On reaching a critical load value, the structure suddenly experiences a large deformation and it may lose its ability to carry the load. At this stage, the structure is considered to have buckled. Buckling, also known as structural instability may be classified into two categories:

a) Bifurcation buckling
b) Limit load buckling

In bifurcation buckling, the deflection under compressive load changes from one
direction to a different direction (e.g., from axial shortening to lateral deflection). In limit load buckling, the structure attains a maximum load without any previous
bifurcation, i.e., with only a single mode of deflection.

2. LITERATURE REVIEW

Leissa AW, Kang JH. Exact solution for buckling of thin plates:

Leissa and Kang used power series (i.e., method of Frobenius) method to obtain the buckling load of the plate with linearly varying in-plane loads .The problem of buckling of a rectangular plate subjected to uniformly distributed in-plane compressive loading at each end goes back to the work of Bryan in 1890–91. The same problem, for the case of linearly varying in-plane compressive loading at each end, was first treated by several European investigators about 90 years ago. The case of loading that is nonlinearly distributed along two opposite plate edges is considerably more complicated in that it requires that first the plane elasticity problem be solved to obtain the distribution of in-plane stresses. Then the buckling problem must be solved. This problem was claimed to have been solved by van der Neut in 1958 for a half-sine load distribution and later by Benoy for a parabolic distribution. However, their work was based on an incorrect in-plane stress distribution. Here is presented a solution for the half-sine load distribution on two opposite sides, based on a more realistic in-plane stress distribution.

This distribution shows a decrease (diffusion) in axial stress as the distance from the loaded edges is increased. The buckling loads are calculated using Galerkin method and the results are compared with the inaccurate results in the literature.

Sarat Kumar Panda, L.S.Ramachandra :[2010]

In this paper, buckling loads of rectangular composite plates having nine sets of different boundary conditions and subjected to non-uniform inplane loading are presented considering higher order shear deformation theory (HSDT). As the applied inplane load is non-uniform, the buckling load is evaluated in two steps. In the first step the plane elasticity problem is solved to evaluate the stress distribution within the pre-buckling range. Using the above stress distribution the plate buckling equations are derived from the principle of minimum total potential energy. Adopting Galerkin's approximation, the governing partial differential equations are converted into a set of homogeneous linear algebraic equations. The critical buckling load is obtained from the solution of the associated linear eigenvalue problem. The present buckling loads are compared with the published results wherever available. The buckling loads obtained from the present method for plate with various boundary conditions and subjected to non-uniform inplane

loading are found to be in excellent agreement with those obtained from commercial software ANSYS. Buckling mode shapes of plate for different boundary conditions with non-uniform inplane loadings are also presented.

It is observed from the literature that, a large volume of research work (Timoshenko and Gere, 1963; Murray and Wilson, 1969; Ng et al., 1998; Ganapathi et al., 1999; Leissa and Kang, 2002;) exists in the area of buckling, postbuckling, dynamic instability of composite plates and shell panels. However, it is observed that stability analysis of plates under non-uniform in-plane loading is scarcely available in the literature (Bert and Devarakonda, 2003; Wang et al., 2007; Zhong and Gu, 2006; Jana and Bhaskar, 2006).

To the best of author's knowledge no work has been carried out in literature on the static stability and dynamic stability of composite plates subjected to non-uniform in-plane loading.Wang have adopted Galerkin procedure with Legendre polynomials as shape function to analyse buckling of rectangular plates subjected to linearly varying inplane edge compressive load with two loaded edges simply supported, one side free and the other side simply supported, clamped or rotationally restrained. Biggers and his co-workers have exploited the stiffness-tailoring concept to improve the buckling load capacity of plates subjected to, compressive load and shear load Whereas, Baranski and Biggers have used the same concept to study the postbuckling response of damaged compo- site plates.

In a companion paper Xie and Biggers have extended the stiffness-tailoring concept to improve the compres- sive buckling loads and ultimate loads of flat pates and curved panels with cutouts. Buckling of moderately thick composite plates subjected to partial edge compression was studied by Sundaresan within the framework of finite element method. presented exact solutions for the Kirchhoff plate having two opposite edges simply supported subjected to linearly varying inplane loading. They have considered all other possible boundary conditions on the unloaded edges. As the loaded edge is simply supported, authors assumed the transverse displacement (w) to vary as sin((mpx)/a) (where a is the size of the plate along x-direction and b along y-direction) and reduced the governing partial differential equation to an ordinary differential equation in y with variable coefficients,for which an exact solution was obtained in terms of power series. Applying the boundary conditions at y=0 and b yields the eigenvalue problem for finding the buckling load.

3. MATHEMATICAL FORMULATION

3.1 The Governing equation

We consider the classical thin plate theory (CPT) in deriving the governing equation, which is based on the Kirchhoff hypothesis:

(a) Straight lines perpendicular to the mid-surface (i.e., transverse normals) before deformation remain straight after deformation.

(b)The transversenormals do not experience elongation (i.e., they are inextensible).

(c)The transverse normals rotate such that they remain perpendicular to the mid-surface after deformation.

The governing partial differential equation defining the lateral deflection of the middle surface of the plate in terms of the applied transverse load is obtained by,

$$\frac{\partial^4 \omega}{\partial x^4} + 2\frac{\partial^4 \omega}{\partial x^2 \partial y^2} + \frac{\partial^4 \omega}{\partial y^4} - \frac{1}{D}\left(N_x \frac{\partial^4 \omega}{\partial x^4} + N_y \frac{\partial^4 \omega}{\partial y^4} + 2N_{xy}\frac{\partial^4 \omega}{\partial x^2 \partial y^2}\right) = 0$$

the determination of the deflection surface of a plate is reduced to the integration of this Equation.

3.2 THE VON KARMAN THEORY OF PLATES

In this section we shall derive the von karman theory of plates. This is a nonlinear theory that allows for comparatively large rotations of line elements originally normal to the x,y axes in the midplane of the plate (figure 1). These rotations terms allow projections of the in- plane forces $\overline{N_v}$ and $\overline{N_{vs}}$ to be felt in the transverse direction, normal to the plane of plate.

This theory is derive assuming that strains and rotations are both small compared to unity, so that we can ignore changes in geometry in the definition of stress components and in the limits of integration needed for work and energy considerations. We further stipulate that the strains will be smaller than the rotations, in the sense described below.

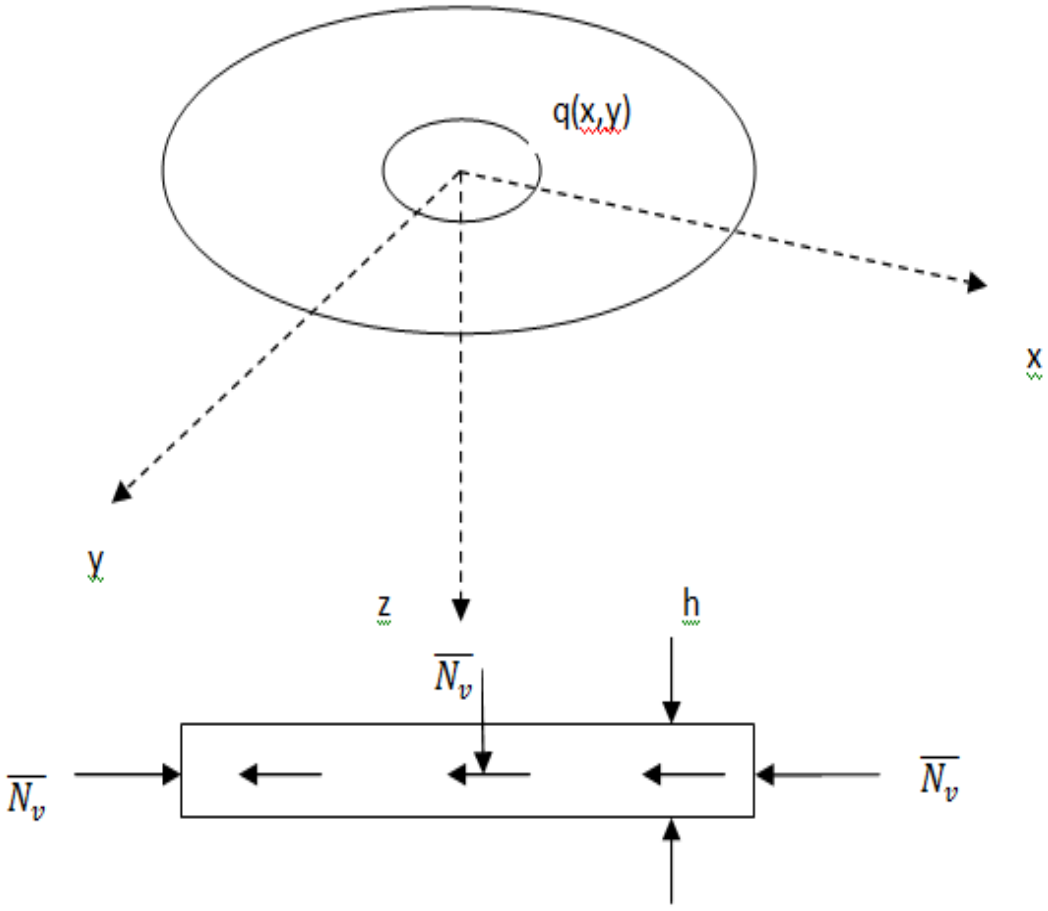

We introduce the linear strain parameters $e_{ij}$and the rotation parameters ω_{ij} defined as

$2e_{ij} = u_{i,j} + u_{j,i}$ (1)

$2\omega_{ij} = u_{i,j} - u_{j,i}$ (2)

$2 \in_{ij} = 2e_{ij} + (e_{ki} + \omega_{ki})(e_{kj} + \omega_{kj})$ (3)

For simplification discussed, namely $e_{ki} << w_{ki}$ reduces to

$\in_{ij} = e_{ij} + \frac{1}{2}\omega_{ki} * \omega_{ki}$ (4)

Finally Kirchhoff assumption that lines normal to under formed middle surface remain normal to this surface in the deformed geometry and are un extended after deformation. That means

$u_1(x_1, x_2, x_3) = u(x,y) - z\frac{\partial w(x,y)}{\partial x}$ (5)

$u_2(x_1, x_2, x_3) = v(x,y) - z\frac{\partial w(x,y)}{\partial y}$ (6)

$u_3(x_1, x_2, x_3) = w(x,y)$ (7)

Where u, v and w are the displacement components of the middle surface of the plate. We may now give strain parameters and rotation parameters as follows:

$e_{11} = \frac{\partial u}{\partial x} - z\frac{\partial^2 w}{\partial x^2}$

$e_{12} = \frac{1}{2}\left(\frac{\partial u}{\partial y} + \frac{\partial v}{\partial x} - 2z\frac{\partial^2 w}{\partial x \partial y}\right)$

$e_{22} = \frac{\partial v}{\partial y} - z\frac{\partial^2 w}{\partial y^2}$ (8a)

$e_{13} = e_{23} = 0$

$\omega_{12} = \frac{1}{2}\left(\frac{\partial u}{\partial y} - \frac{\partial v}{\partial x}\right)$

$\omega_{13} = -\frac{\partial w}{\partial x}$ (8b)

$\omega_{23} = -\frac{\partial w}{\partial y}$

We now observe the following. The rotation parameter ω_{12} approximates a rotation component about the z axis, while rotation components about axes parallel to the x and y axes ,respectively, in the mid plane of the plate. For a thin, hence flexible, plate we can reasonably expect that:

$$\omega_{12} << \omega_{23}, \omega_{13} \tag{9}$$

Neglecting $\omega_{12,}$ we can now employ Eqs. 4 and 8 to find the $\in_{ij}$:

$$\in_{11} = \frac{\partial u}{\partial x} - z\frac{\partial^2 w}{\partial x^2} + \frac{1}{2}\left(\frac{\partial w}{\partial x}\right)^2$$

$$\in_{22} = \frac{\partial v}{\partial y} - z\frac{\partial^2 w}{\partial y^2} + \frac{1}{2}\left(\frac{\partial w}{\partial y}\right)^2$$

$$\in_{33} = \frac{1}{2}\left(\frac{\partial w}{\partial x}\right)^2 + \frac{1}{2}\left(\frac{\partial w}{\partial y}\right)^2 \tag{10}$$

$$\in_{12} = \frac{1}{2}\left(\frac{\partial u}{\partial y} + \frac{\partial v}{\partial x} - 2z\frac{\partial^2 w}{\partial x \partial y}\right) + \frac{1}{2}\frac{\partial w}{\partial x}\frac{\partial w}{\partial y}$$

$$\in_{13} \cong \in_{23} \cong 0$$

For a constitutive law we will employ Hook's law for plane stress over the thickness of the plate. Thus we shall be concerned here only with $\in_{11}$, $\in_{22}$ and $\in_{12}$. Accordingly , for the assumptions presented here, we can say that the first variation of strain energy U is

$$\delta^{(1)}U = \iiint_V \tau_{ij}\ \delta \in_{ij} dv = \iint_R \int_{-h/2}^{h/2} (\tau_{11}\,\delta \in_{11} + 2\tau_{12}\delta \in_{12} + \tau_{22}\delta \in_{22}) dz\, dA \tag{11}$$

Now we replace the strain terms in the above expression and commute the delta operator with derivative operators.

$$\delta^{(1)}U = \iint_R \int_{-h/2}^{h/2} \{\left[\tau_{11}\left(\frac{\partial\,\delta u}{\partial x} + \frac{\partial w}{\partial x}\frac{\partial\,\delta w}{\partial x} - z\frac{\partial^2\,\delta w}{\partial x^2}\right)\right] + \left(\frac{\partial\,\delta u}{\partial y} + \frac{\partial\,\delta v}{\partial x} - 2z\frac{\partial^2\,\delta w}{\partial x \partial y} + \frac{\partial w}{\partial x}\frac{\partial\,\delta w}{\partial y} + \frac{\partial w}{\partial y}\frac{\partial\,\delta w}{\partial x}\right)$$
$$+\tau_{22}\left(\frac{\partial\,\delta v}{\partial y} + \frac{\partial w}{\partial y}\frac{\partial\,\delta w}{\partial y} - z\frac{\partial^2\,\delta w}{\partial y^2}\right)\} dA\, dz \tag{12}$$

Next we integrate with respect to z and introduce resultant stress and moment intensity functions N_x, N_y and N_{xy}, and M_x, M_y, $and\ M_{xy}\ respectively$:

$$M_x = \int_{-h/2}^{h/2} \tau_{xx} z\, dz$$

$$M_y = \int_{-h/2}^{h/2} \tau_{yy} z \, dz$$

$$M_{xy} = \int_{-h/2}^{h/2} \tau_{xx} z \, dz = M_{xy} \quad (13)$$

$$N_x = \int_{-h/2}^{h/2} \tau_{xx} \, dz$$

$$N_y = \int_{-h/2}^{h/2} \tau_{yy} \, dz$$

$$N_{xy} = \int_{-h/2}^{h/2} \tau_{xy} \, dz = N_{yx} \quad (14)$$

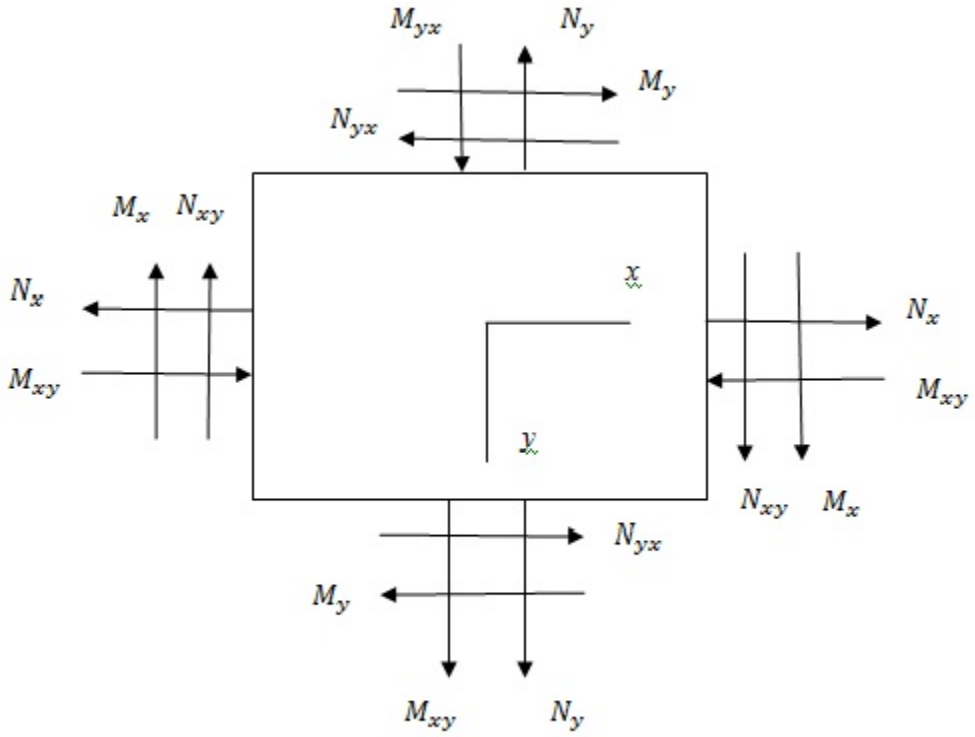

Figure 2

Where N_x (N_y), as shown in the figure2 is a force in the x direction (y direction) measured per unit length in the y direction (x direction) and where N_{xy} (N_{yx}) is a force in the x(y) direction per unit length in the y(x) direction. Similarly, the quantity M_x represents a moment per unit length in the y direction, with its vector in the y direction. Finally, M_{xy} is the twisting moment per unit length in the y direction with its vector in the x direction. The terms $N_{x,}$ $N_{y,}$ N_{xy} and N_{yx} may

for practical purposes be compared with normal and shear stresses and we may conclude that $N_{xy} = N_{yx}$ then we got the following result:

The Eqs 12 can be written as

$$\delta^{(1)}U = \iint_R \left[N_x \left(\frac{\partial\, \delta u}{\partial x} + \frac{\partial w}{\partial x}\frac{\partial\, \delta w}{\partial x}\right) - M_x \frac{\partial^2\, \delta w}{\partial x^2} + N_{xy} \left(\frac{\partial\, \delta u}{\partial y} + \frac{\partial\, \delta v}{\partial x} + \frac{\partial w}{\partial x}\frac{\partial\, \delta w}{\partial y} + \frac{\partial w}{\partial y}\frac{\partial\, \delta w}{\partial x}\right) - 2M_{xy} \frac{\partial^2\, \delta w}{\partial x \partial y} + N_y \left(\frac{\partial\, \delta v}{\partial y} + \frac{\partial w}{\partial y}\frac{\partial\, \delta w}{\partial y}\right) - M_y \frac{\partial^2\, \delta w}{\partial y^2}\right] \mathrm{dx\ dy} \qquad (14)$$

The first variation of the potential of the applied forces meanwhile takes the form (noting that $\overline{N_v}$ is taken as positive in compression as shown in the figure.

$$\delta^{(1)}V = -\iint_R q\ \delta w\ dx\ dy + \oint_r \overline{N_v}\ \delta u_v\ ds + \oint_r \overline{N_{vs}}\ \delta u_s\ ds \qquad (15)$$

Where u_v and u_s are the in plane displacements of the boundary of the plate in direction normal and tangential to the boundary, respectively. We are using the under formed geometry for the applied loads above rather than the deformed geometry thereby restricting the result to reasonably small deformations. By using the above result for $\delta^{(1)}V$ and using equation 14 for $\delta^{(1)}U$, may be form $\delta^{(1)}\pi$. the total potential energy so formed approximates the actual total potential energy for the kind of deformation restrictions embodied in kirchhoff's assumptions. And since we have used undeformed geometry for stresses and external loads, we are limited to small deformations in employing this functional. Finally, because we used equation 4 for strain, we are assuming that strains are much smaller than rotations. Thus we have for the total potential energy principle:

$$\delta^{(1)}\pi = \mathrm{U} = \iint_R \left[N_x \left(\frac{\partial\, \delta u}{\partial x} + \frac{\partial w}{\partial x}\frac{\partial\, \delta w}{\partial x}\right) - M_x \frac{\partial^2\, \delta w}{\partial x^2} + N_{xy} \left(\frac{\partial\, \delta u}{\partial y} + \frac{\partial\, \delta v}{\partial x} + \frac{\partial w}{\partial x}\frac{\partial\, \delta w}{\partial y} + \frac{\partial w}{\partial y}\frac{\partial\, \delta w}{\partial x}\right) - 2M_{xy} \frac{\partial^2\, \delta w}{\partial x \partial y} + N_y \left(\frac{\partial\, \delta v}{\partial y} + \frac{\partial w}{\partial y}\frac{\partial\, \delta w}{\partial y}\right) - M_y \frac{\partial^2\, \delta w}{\partial y^2}\right] \mathrm{dx\ dy} - \iint_R q\ \delta w\ dx\ dy + \oint_r \overline{N_v}\ \delta u_v\ ds + \oint_r \overline{N_{vs}}\ \delta u_s\ ds \qquad (16)$$

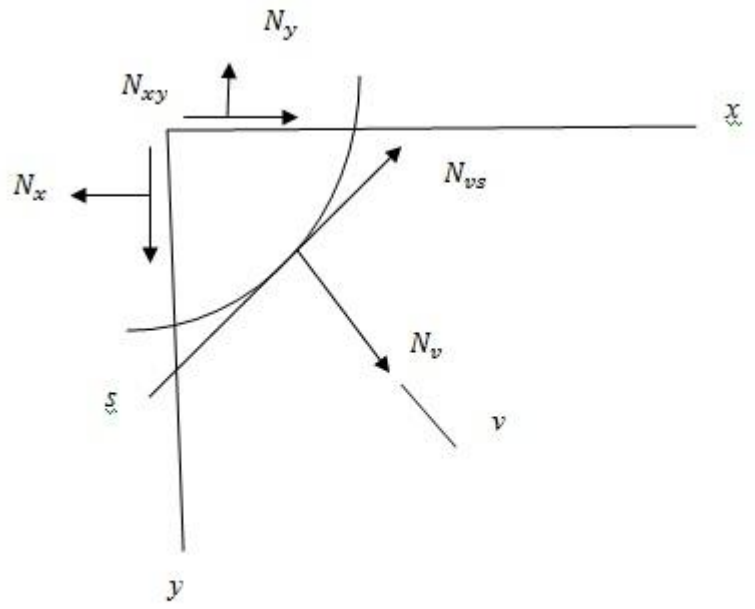

Figure3

We may proceed to carry out the extermination process. We employ Green's theorem one or more times to get the $\delta u's$ and $\delta v's$ out form of partial derivatives. Then we proceed to simplify the expressions in the line integrals by noting form equilibrium shown in the above figure3.

$$N_v = N_x\ a^2{}_{vx} + 2N_{xy}a_{vx}a_{vy} + N_y\ a^2{}_{vy} \tag{17}$$

$$N_{vs} = (N_y - N_x) + 2N_{xy}a_{vx}a_{vy} + N_{xy}(\ a^2{}_{vx} - a^2{}_{vy}) \tag{18}$$

Where a_{vx} and a_{vy} are the direction cosine of the outward normal of the boundary. Furthermore, simple vector projections permit us to say

$$u_v = a_{vx}\mathrm{u} + a_{vy}\mathrm{v} \tag{19}$$

$$u_s = -a_{vy}\mathrm{u} + a_{vx}\mathrm{v} \tag{20}$$

Here we also note

$$\frac{\partial}{\partial x} = a_{vx}\frac{\partial}{\partial v} - a_{vy}\frac{\partial}{\partial s} \tag{21}$$

$$\frac{\partial}{\partial y} = a_{vy}\frac{\partial}{\partial v} + a_{vx}\frac{\partial}{\partial s} \qquad (22)$$

Finally we introduce the transverse shear forces of plate theory

$$Q_v = Q_x a_{vx} + Q_y a_{vy}$$

$$Q_x = \frac{\partial M_x}{\partial x} + \frac{\partial M_{xy}}{\partial y} \qquad (23)$$

$$Q_y = \frac{\partial M_y}{\partial y} + \frac{\partial M_{xy}}{\partial x}$$

Now using equation 17, 18 and 23 we can write as

$$\delta^{(1)}\pi = -\iint_R \left[\left(\frac{\partial N_x}{\partial x} + \frac{\partial N_{xy}}{\partial y}\right)\delta u + \left(\frac{\partial N_{xy}}{\partial x} + \frac{\partial N_y}{\partial y}\right)\delta v + \left\{\frac{\partial^2 M_x}{\partial x^2} + 2\frac{\partial^2 M_{xy}}{\partial x \partial y} + \frac{\partial^2 M_y}{\partial y^2} + \frac{\partial}{\partial x}\left(N_x\frac{\partial w}{\partial x}\right) + \frac{\partial}{\partial y}\left(N_{xy}\frac{\partial w}{\partial x}\right) + \frac{\partial}{\partial x}\left(N_{xy}\frac{\partial w}{\partial y}\right) + \frac{\partial}{\partial y}\left(N_y\frac{\partial w}{\partial y}\right) + q\right\}\delta w\right]\mathrm{dx\ dy} + \oint_r (N_v + \overline{N_v})\delta u_v\, ds + \oint_r (N_{vs} + \overline{N_{vs}})\delta u_s\, ds - \oint_r M_v\frac{\partial \delta w}{\partial v}\, ds + \oint_r \left(Q_v + \frac{\partial M_{vs}}{\partial s} + N_v\frac{\partial w}{\partial v} + N_{vs}\frac{\partial w}{\partial s}\right)\delta w\, ds - [M_{vs}\,\delta w]_r = 0 \quad \ldots..(24)$$

The last expression accounts for "corners" in the boundary. From the above equations we may now make series of deductions. First, in region R we conclude that

$$\frac{\partial N_x}{\partial x} + \frac{\partial N_{xy}}{\partial y} = 0 \qquad (25a)$$

$$\frac{\partial N_{xy}}{\partial x} + \frac{\partial N_y}{\partial y} = 0 \qquad (25b)$$

$$\frac{\partial^2 M_x}{\partial x^2} + 2\frac{\partial^2 M_{xy}}{\partial x \partial y} + \frac{\partial^2 M_y}{\partial y^2} + \frac{\partial}{\partial y}\left(N_x\frac{\partial w}{\partial x}\right) + \frac{\partial}{\partial y}\left(N_{xy}\frac{\partial w}{\partial x}\right) + \frac{\partial}{\partial x}\left(N_{xy}\frac{\partial w}{\partial y}\right) + \frac{\partial}{\partial y}\left(N_y\frac{\partial w}{\partial y}\right) + q = 0 \qquad (25c)$$

The first two equations above clearly are identical to the equations of equilibrium for plane stress, as is to be expected. We shall use these equations now to simplify the third equation after we use the differentiation operators on the above expressions involving products. We are thus able to eliminate expressions involving products. We are thus able to eliminate expressions involving products. We are thus able to eliminate expressions involving the partial of w.We get

$$\frac{\partial^2 M_x}{\partial x^2} + 2\frac{\partial^2 M_{xy}}{\partial x \partial y} + \frac{\partial^2 M_y}{\partial y^2} + N_x \frac{\partial^2 w}{\partial x^2} + 2N_{xy}\frac{\partial^2 w}{\partial x \partial y} + N_y \frac{\partial^2 w}{\partial y^2} + q = 0 \qquad (26)$$

Now comparing Eq. 26 with the classical case we have here introduced nonlinear terms $\left[N_x \frac{\partial^2 w}{\partial x^2} + 2N_{xy}\frac{\partial^2 w}{\partial x \partial y} + N_y \frac{\partial^2 w}{\partial y^2}\right]$ involving the in-plane force intensities as additional "transverse loading".

Considering next the reminder Eq. (24) we can stipulate the following boundary conditions along Γ:

EITHER N_v = -$\overline{N_v}$ OR u_v IS SPECIFIED (27a)

EITHER N_{vs} = -$\overline{N_{vs}}$ OR u_s IS SPECIFIED (27b)

EITHER M_v = 0 OR $\frac{\partial w}{\partial v}$ IS SPECIFIED (27c)

EITHER $Q_v + \frac{\partial M_{vs}}{\partial s} + N_v \frac{\partial w}{\partial v} + N_{vs}\frac{\partial w}{\partial s}$ = 0 OR w IS SPECIFIED (27d)

At discontinuities $[M_{vs}\,\delta w] = 0$ (27e)

The last three conditions are familiar form work on plates except that the effective shear force ($Q_v + \frac{\partial M_{vs}}{\partial s}$) is now augmented by projections of the in-plate forces at the plate edges.

The equations of equilibrium may be solved if a constitutive law is used. We will employ here (as pointed out earlier) the familiar Hook's law for plane stress. We will use the constitutive law to replace the resultant intensity functions by appropriate derivatives of the displacement field of the mid plane of the plate. Consider, for example, the quantity M_x. Using Hook's law and Eq. (10), we have

$$M_x = \int_{-h/2}^{h/2} \tau_{xx} z\, dz = \int_{-h/2}^{h/2} z \frac{E}{1-\mu^2}\,(\in_{xx} + \mu \in_{yy}) dz = \int_{-h/2}^{h/2} z \frac{E}{1-\mu^2}\left[\frac{\partial u}{\partial x} - z\frac{\partial^2 w}{\partial x^2} + \frac{1}{2}\left(\frac{\partial w}{\partial x}\right)^2 + \mu\,\frac{\partial v}{\partial y} - z\mu\frac{\partial^2 w}{\partial y^2} + \frac{\mu}{2}\left(\frac{\partial w}{\partial y}\right)^2\right] dz$$

Integrating and inserting limits, we get

$$M_x = \frac{E}{1-\mu^2}\,\frac{h^3}{12}\left(-\frac{\partial^2 w}{\partial x^2} - \mu\frac{\partial^2 w}{\partial y^2}\right) = -\mathrm{D}\left(\frac{\partial^2 w}{\partial x^2} + \mu\frac{\partial^2 w}{\partial y^2}\right) \quad (28)$$

Where D is the familiar bending rigidity, given as $\mathrm{D} = \frac{Eh^3}{12(1-\mu^2)}$, similarly we have

$$M_y = -\mathrm{D}\left(\frac{\partial^2 w}{\partial y^2} + \mu\frac{\partial^2 w}{\partial x^2}\right) \quad (29a)$$

$$M_{xy} = -\,\mathrm{D}(1-\mu)\,\frac{\partial^2 w}{\partial x \partial y} \quad (29b)$$

$$N_y = \mathrm{C}\left\{\left[\frac{\partial u}{\partial x} + \frac{1}{2}\left(\frac{\partial w}{\partial x}\right)^2\right] + \mu\left[\frac{\partial v}{\partial y} + \frac{1}{2}\left(\frac{\partial w}{\partial y}\right)^2\right]\right\} \quad (29c)$$

$$N_x = \mathrm{C}\left\{\left[\frac{\partial v}{\partial y} + \frac{1}{2}\left(\frac{\partial w}{\partial y}\right)^2\right] + \mu\left[\frac{\partial u}{\partial x} + \frac{1}{2}\left(\frac{\partial w}{\partial x}\right)^2\right]\right\} \quad (29d)$$

$$N_{xy} = \mathrm{C}\left(\frac{1-\mu}{2}\right)\left[\frac{\partial u}{\partial y} + \frac{\partial v}{\partial x} + \frac{\partial w}{\partial x}\frac{\partial w}{\partial y}\right] \quad (29e)$$

Where C is given extensional rigidity, given as

$$\mathrm{C} = \frac{Eh}{1-\mu^2}$$

We could now substitute in Eq. (26) for the resultant intensity functions, using above relations to get the equilibrium equations in terms of displacement components of the mid plane plate. However, we shall follow another route that leads to a somewhat less complicated system of equations.

Note accordingly that Eqs. (25a) and (25b) will be individually satisfied if we define an Airy stress function F as follows:

$$N_x = \frac{\partial^2 F}{\partial y^2}$$

$$N_y = \frac{\partial^2 F}{\partial x^2} \quad (30)$$

$$N_{xy} = -\frac{\partial^2 F}{\partial x\,\partial y}$$

Then, replacing, and, it is a simple matter to show that Eq. (25c) can be written as

$$D\nabla^4 w = \frac{\partial^2 F}{\partial y^2}\frac{\partial^2 w}{\partial x^2} - 2\frac{\partial^2 F}{\partial x\,\partial y}\frac{\partial^2 w}{\partial x\,\partial y} + \frac{\partial^2 F}{\partial x^2}\frac{\partial^2 w}{\partial y^2} + q \qquad (31)$$

We now have a single partial differential equation with two dependent variables, w and F. since we are now studying in-plane effects by a stress approach, we must ensure the compatibility of the in-plane displacements. This will give us a second companion equation to go with Eq. (31). To do this, we shall seek to relate the strain $\epsilon_{xx,}$ $\epsilon_{yy,}$ and ϵ_{xy} at the mid plane surface in such a way that when employ Eq. (10) to replace the strains we end up with a result that does not contain the in-plane displacement components *u* and *v*. thus we you may readily demonstrate by substituting from Eq. (10) that

$$\left(\frac{\partial^2 \epsilon_{xx}}{\partial y^2} - 2\frac{\partial^2 \epsilon_{xy}}{\partial x \partial y} + \frac{\partial^2 \epsilon_{yy}}{\partial x^2}\right)_{z=0} = \left(\frac{\partial^2 w}{\partial x\,\partial y}\right)^2 - \frac{\partial^2 w}{\partial x^2}\frac{\partial^2 w}{\partial y^2} \qquad (32)$$

Since this equation ensures the proper relation of strains at the mid plane surface to the mid plane displacement component *w* without explicitly involving in-plane displacement components *u* and *v*, it serves as the desired compatibility equation for the strains at the mid plane surface. We next express the compatibility equation in terms of the stress resultant intensity function. To do this, substitute for strains, using Eq.(10) and then note Eqs.(29) stemming from Hook's law:

$$\frac{1}{Eh}\left[\frac{\partial^2 N_x}{\partial y^2} - \mu\frac{\partial^2 N_y}{\partial y^2} + \frac{\partial^2 N_y}{\partial x^2} - \mu\frac{\partial^2 N_x}{\partial x^2} + 2(1+\mu)\frac{\partial^2 N_{xy}}{\partial x \partial y}\right] = \left(\frac{\partial^2 w}{\partial x\,\partial y}\right)^2 - \frac{\partial^2 w}{\partial x^2}\frac{\partial^2 w}{\partial y^2}$$

Finally, replacing the resultant intensity functions in terms of the Airy function [see Eq. (30)], we get

$$\nabla^4 F = Eh\left[\left(\frac{\partial^2 w}{\partial x\,\partial y}\right)^2 - \frac{\partial^2 w}{\partial x^2}\frac{\partial^2 w}{\partial y^2}\right] \qquad (33)$$

the above equation and Eq. (), which we now rewrite as

$$D\,\nabla^4 w = \frac{\partial^2 F}{\partial y^2}\frac{\partial^2 w}{\partial x^2} - 2\frac{\partial^2 F}{\partial x\,\partial y}\frac{\partial^2 w}{\partial x\,\partial y} + \frac{\partial^2 F}{\partial x^2}\frac{\partial^2 w}{\partial y^2} + q \qquad (34)$$

Are the celebrated von karman plate equations. Note that they are still highly non-linear. The equations do have considerable mutual symmetry. This is brought out by defining a nonlinear operator L:

$$L(p,q) = \frac{\partial^2 p}{\partial y^2}\frac{\partial^2 q}{\partial x^2} - 2\frac{\partial^2 p}{\partial x\,\partial y}\frac{\partial^2 q}{\partial x\,\partial y} + \frac{\partial^2 p}{\partial x^2}\frac{\partial^2 q}{\partial y^2} \quad (35)$$

Then the von karman plate equations can be given as

$$\nabla^4 F = -\frac{Eh}{2} L(w,w) \quad (36a)$$

$$D\,\nabla^4 w = L(F,w) + q \quad (36b)$$

The deflection of the non linear operator leaves us with the (uncoupled) plane –stress problem of two – dimensional elasticity theory and the classic plate bending equation.

3.3 BOUNDARY CONDITIONS

A complete solution of the governing Equation depends upon the knowledge of conditions of the plate at the boundaries in terms of the lateral deflection of the middle surface *w(x, y).* The critical buckling load of composite rectangular plate with various boundary conditions and subjected to parabolically varying in plane compressive load is obtained using Galerkin's method. In the present investigation following nine sets of boundary conditions are considered :SSSS, SSCS, SCSS, CSCS, SCSC, SSCC, CCSC, CCCS and CCCC, where S stands for simply supported edge and C for clamped edge. The letters indicate the boundary conditions on the edge of the plate in the anti-clockwise fashion starting from the left hand corner. In the Galerkin's method, the out-of-plane displacement field w(x,y) satisfying the boundary conditions of the plate is expressed as the product of beam function as

$$\omega = \sum_{m=1}^{\infty}\sum_{n=1}^{\infty} X_m(x) Y_n(y)$$

Where $X_m(x)$ and $Y_n(y)$ are the eigen functions of the beam having the same boundary conditions as that of two opposite edges of the plate.This choice of functions satisfies all boundary conditions of the plate exactly.In present case following beam functions are adopted:.

3.3.1 Simply Supported along two opposite Edges at x=0 and x=a:

A plate boundary that is prevented from deflecting but free to rotate about a line along the boundary edge, such as a hinge, is defined as a simply supported edge. The conditions on a simply supported edge paralled to the y-axis at $x = a$, are.

$$X_m^{ss}(x) = sin\frac{m\pi x}{a} \qquad \text{(m=1,2,3…….)}$$

3.3.2 Clamped support along two opposite Edges at x=0 and x=a:

If a plate is clamped, the deflection and the slope of the middle surface must vanish at the boundary. On a clamped edge parallel to the y-axis at $x=0$ and x=a the boundary conditions are,

$$X_m^{cc} = cos\delta\left(\frac{x}{2a} - 0.5\right) + \frac{\sin\left(\frac{\delta}{2}\right)}{\sinh\left(\frac{\delta}{2}\right)} cosh\delta\left(\frac{x}{a} - 0.5\right) \qquad \text{(m=2,4,6,……)}$$

Where δ are obtained as roots of $\tan(\delta/2) + \tanh(\delta/2) = 0$

And

$$X_m^{cc} = sin\delta\left(\frac{x}{2a} - 0.5\right) - \frac{\sin\left(\frac{\delta}{2}\right)}{\sinh\left(\frac{\delta}{2}\right)} cosh\delta\left(\frac{x}{a} - 0.5\right) \qquad \text{(m=3,5,7……)}$$

Where δ are obtained as roots of $\tan(\delta/2) - \tanh(\delta/2) = 0$

3.3.3 Clamped support along the Edge at x=0 and simply supported at x=a:

If a plate is simply supported along two opposite sides and clamped on the other two sides at y=*0*, and y=*b*. The boundary conditions are,

$$X_m^{cs} = sin\delta\left(\frac{x}{2a} - 0.5\right) - \frac{\sin\left(\frac{\delta}{2}\right)}{\sinh\left(\frac{\delta}{2}\right)} sinh\delta\left(\frac{x}{a} - 0.5\right) \qquad \text{(m=2,3,4……..)}$$

Where δ are obtained as roots of $\tan(\delta/2) - \tanh(\delta/2) = 0$

3.4 GALERKIN METHOD

Galerkin's Method, invented by Russian mathematician Boris Grigoryevich Galerkin. In galerkin's method find the function which satisfies the given differential equations and boundary conditions. The Galerkin's method has been used to solve problems in mechanical engineering such as structural mechanics, dynamics, fluid flow, heat and mass transfer, acoustics, neutron transport and others. The Galerkin method can be used to approximate the solution to ordinary differential equations, partial differential equation and integral equations.

- Identify the differential equation to solve, along with its domain and boundary condition.
- Identify the vector space in which to look for a solution called the solution space.
- Rewrite the differential equation in a special way know as weak formulation.
- Decide what type of function are to be used to approximate the solution.
- Solve the resulting weak formulation to reflect this approximating function.
- Solve the resulting weak formulation for an approximate solution.

An approximate solution $(\tilde{u}^o, \tilde{v}^o, \tilde{w}^o)$ of the problem is sought in the form

$$\tilde{u}^o = \sum_{m=1}^{i} \sum_{n=1}^{j} U_{mn} \bar{a}_{mn}(x,y)$$

$$\tilde{v}^o = \sum_{m=1}^{i} \sum_{n=1}^{j} V_{mn} \bar{b}_{mn}(x,y)$$

$$\tilde{w}^o = \sum_{m=1}^{i} \sum_{n=1}^{j} W_{mn} \bar{c}_{mn}(x,y)$$

where $U_{mn,}\ V_{mn} and\ W_{mn}$ are undetermined coefficients and $\bar{a}_{mn}$, $\bar{b}_{mn}$, and $\bar{c}_{mn}$, are suitably chosen spatial functions satisfying the prescribed boundary conditions.

Then the Galerkin method implies

$\iint L_1(\tilde{u}^o, \tilde{v}^o, \tilde{w}^o)\ \bar{a}_{mn}(x,y)dxdy=0$

$\iint L_1(\tilde{u}^o, \tilde{v}^o, \tilde{w}^o)\ \bar{b}_{mn}(x,y)dxdy=0$

$\iint L_1(\tilde{u}^o, \tilde{v}^o, \tilde{w}^o)\ \bar{c}_{mn}(x,y)dxdy=0$

where the integration is carried out over the entire shell area. There will be as many equations (in L_i) as the number of terms taken for the series.

3.5 GALERKIN'S METHOD USED IN PRESENT PROBLEM:

In the present problem first we find out the Governing differential equation by using Von-karman method. Because this problem is only one degree of freedom problem so we use only on approximate solution using Galerkins method.

In the Galerkin's method, the out-of-plane displacement field w(x,y) satisfying the boundary conditions of the plate is expressed as the product of beam function as

$$\omega = \sum_{m=1}^{\infty}\sum_{n=1}^{\infty} X_m(x)Y_n(y)$$

Where $X_m(x)$ and $Y_n(y)$ are the eigen functions of the beam having the same boundary conditions as that of two opposite edges of the plate. This choice of functions satisfies all boundary conditions of the plate exactly. In present case the function used is described in previous article..

Approximate solution for the partial differential equation can be obtain using the Galerkin's method. , In the case of simply supported edges, by the double series,

$$w = \sum_{m=1}^{\infty} \sum_{n=1}^{\infty} a_{mn} \ sin \frac{m\pi x}{a} \ cos \frac{n\pi y}{b}$$

Put this deflection(w) value in Governing differential Equation and find the value Residue(R).

In the present problem the residual is,

$$\frac{\partial^4 \omega}{\partial x^4} + 2\frac{\partial^4 \omega}{\partial x^2 \partial y^2} + \frac{\partial^4 \omega}{\partial y^4} - \frac{1}{D}\left(N_x \frac{\partial^4 \omega}{\partial x^4} + N_y \frac{\partial^4 \omega}{\partial y^4} + 2N_{xy} \frac{\partial^4 \omega}{\partial x^2 \partial y^2}\right) = R$$

after that applying the Galerkin's method:

$$\int_0^a \int_0^b R * sin \frac{m\pi x}{a} \ sin \frac{n\pi y}{b} dx \ dy = 0$$

By this Equation we convert the Governing differential Equation into Algebraic Equation now the problem will be reduced into eigen value problem.

4. RESULT AND DISCUSSION:

In this presentation we find the critical buckling load for different in-plane loadings for different support condition and buckling modes for simply supported plate for different aspect ratio by using Galerkin's method for Uniformly Compressed in One Direction by using the MAT-LAB programming.

The critical buckling load of rectangular plate with various boundary conditions and subjected to parabolically varying inplane compressive load is obtained using Galerkin's method. In the present investigation following nine sets of boundary conditions are considered: SSSS, SSCS, SCSS, CSCS, SCSC, SSCC, CCSC, CCCS and CCCC, where S stands for simply supported edge and C for clamped edge.

We will also use the MAT LAB programming to finding the eigen value for the Algebric Equation which gives the critical buckling load. We will plot the graph between aspect ration (a/b) and the factor (k) by using the Mat-lab programming and find the different modes for different aspect ratio. To change the inplane loading condition taking a linearly varying loads in the form:

$$N_{xx} = N_{xcr}[1\text{-}\alpha\,(\frac{y}{b})] \qquad \{ y= (0,b)\}$$

By taking various values of α, we obtain different inplane load distribution uniform (α=0), trapezoidal (α=0.5), triangular (α=1), partial tension (α=1.5) and pure bending (α=2.0).After evaluating the constants α_i (i=1,2,3), the stress distribution with in the plate are obtained.

The critical buckling load is given by

$$\bar{N}_{xcr} = 4\frac{\pi^2 D}{b^2}$$

For other proportions of the plate the $\bar{N}_x$ can be represented in the form

$$\bar{N}_x = \frac{k\pi^2 D}{b^2}$$

Where k is a numerical factor ,

4.1 Buckling of simply supported rectangular plate with different type of inplane loading:

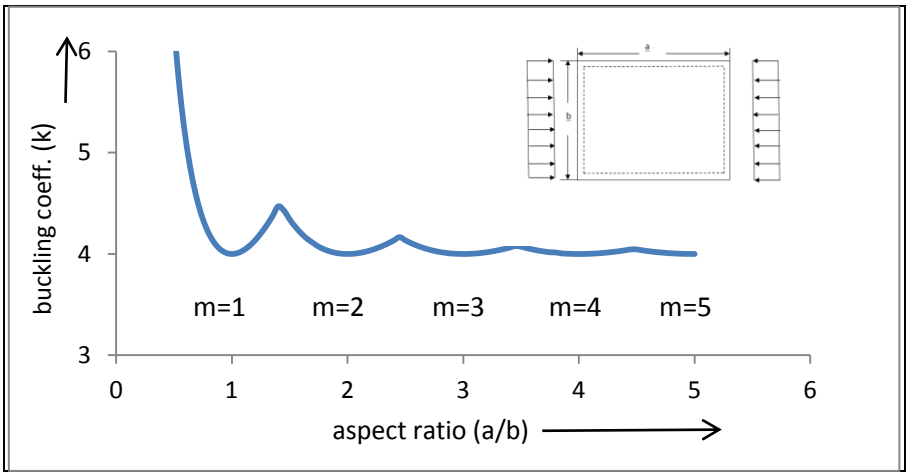

Fig.1 Variation of buckling coefficients of SSSS plate with the aspect ratio(a/b)

The variation of dimensionless buckling load coefficients of a isotropic plate with all simply supported edges subjected to linearly varying inplane load against aspect ratio(a/b) of the plate is shown in figure1. In the graph shows that if we increase the aspect ratio (0 to 5) of the plate , different modes are found. Buckling modes changes from m=1 to m=2 at aspect ratio (a/b=$\sqrt{2}$). similarly the mode changes from m=2 to m=3 at aspect ratio (a/b =$\sqrt{6}$). Modes changes from m=3 to m=4 at aspect ratio(a/b=$\sqrt{12}$) & Modes changes from m=4 to m=5 at aspect ratio (a/b= $\sqrt{20}$). It is observed from the figure1 that for very long (a/b>5) plates, the buckling loads remains the same.The results are exactly matching with the results given in Timoshenko S.P and Gere J.M. "Theory of elastic stability".

The variation of dimensionless buckling load coefficients of a isotropic plate with all simply supported edges subjected to trapezoidal inplane load against aspect ratio(a/b) of the plate is shown in figure2. In the graph shows that if we increase the aspect ratio (0 to 5) of the plate , different modes are found. In point where aspect ratio is (a/b=1.4) ,the mode of the plate are changed from m=1 to m=2.similarly the aspect ratio (a/b =2.45,3.45 & 4.45) points are changed the different modes. It is observed from the figure that for very long (a/b>5) plates, the buckling loads remains the same but the deflection curve is going sharp.

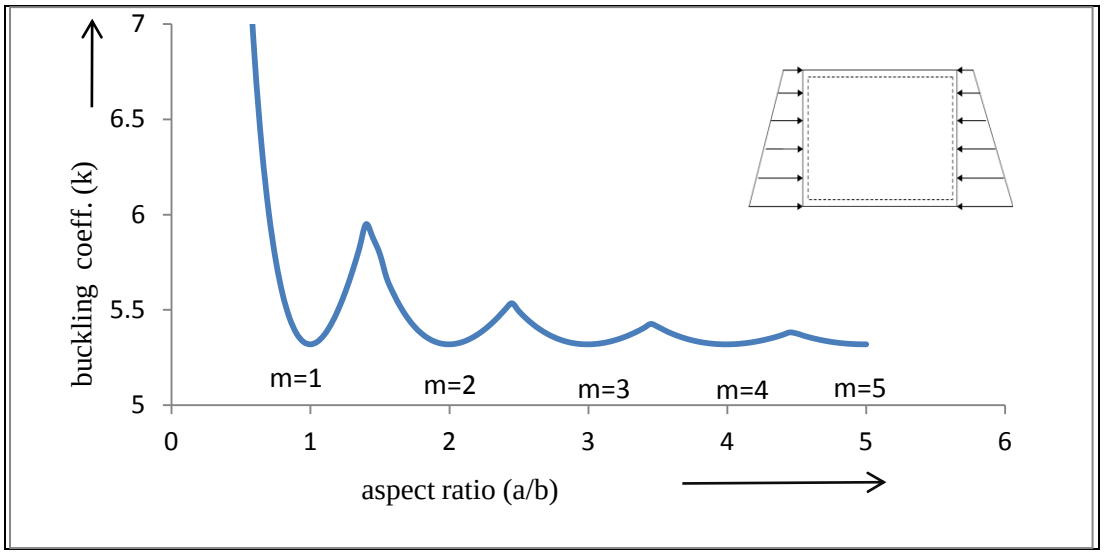

Fig.2 Variation of buckling coefficients of SSSS plate with the aspect ratio (a/b)

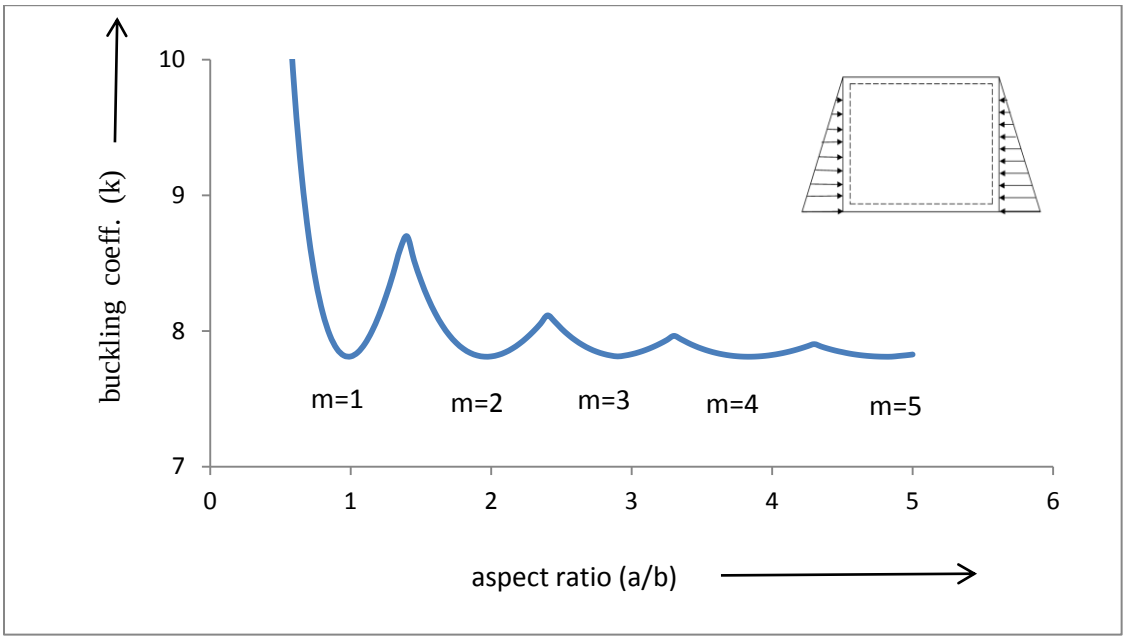

Fig.3 Variation of buckling coefficients of SSSS plate with the aspect ratio (a/b)

The variation of dimensionless buckling load coefficients of a isotropic plate with all simply supported edges subjected to triangular inplane load against aspect ratio(a/b) of the plate is shown in figure 3. In the graph shows that if we increase the aspect ratio (0 to 5) of the plate , different modes are found. In point where aspect ratio is (a/b=1.45) ,the mode of the plate are changed from m=1 to m=2.similarly the aspect ratio (a/b =2.4,3.3 & 4.3) points are changed the different modes. It is observed from the figure that for very long (a/b>5) plates, the buckling loads remains the same.

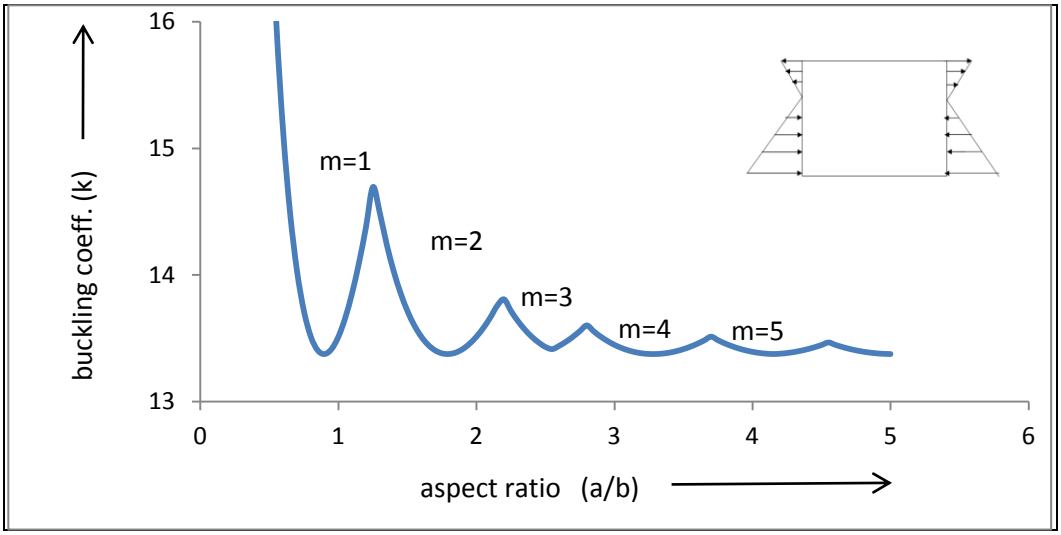

Fig.4 Variation of buckling coefficients of SSSS plate with the aspect ratio (a/b)

In the Fig.4 shows that if we increase the aspect ratio (0 to 5) of the plate , different modes are found. In point where aspect ratio is (a/b=1.25) ,the mode of the plate are changed from m=1 to m=2.similarly the aspect ratio (a/b =2.20,2.85,3.70 & 4.55) points are changed the different modes. In this loading we seen that the more number of modes are obtained, means the variation in loading from the one end to other end of the plate gives more effect in buckling. It is observed from the figure that for very long (a/b>5) plates, the buckling loads remains the same.

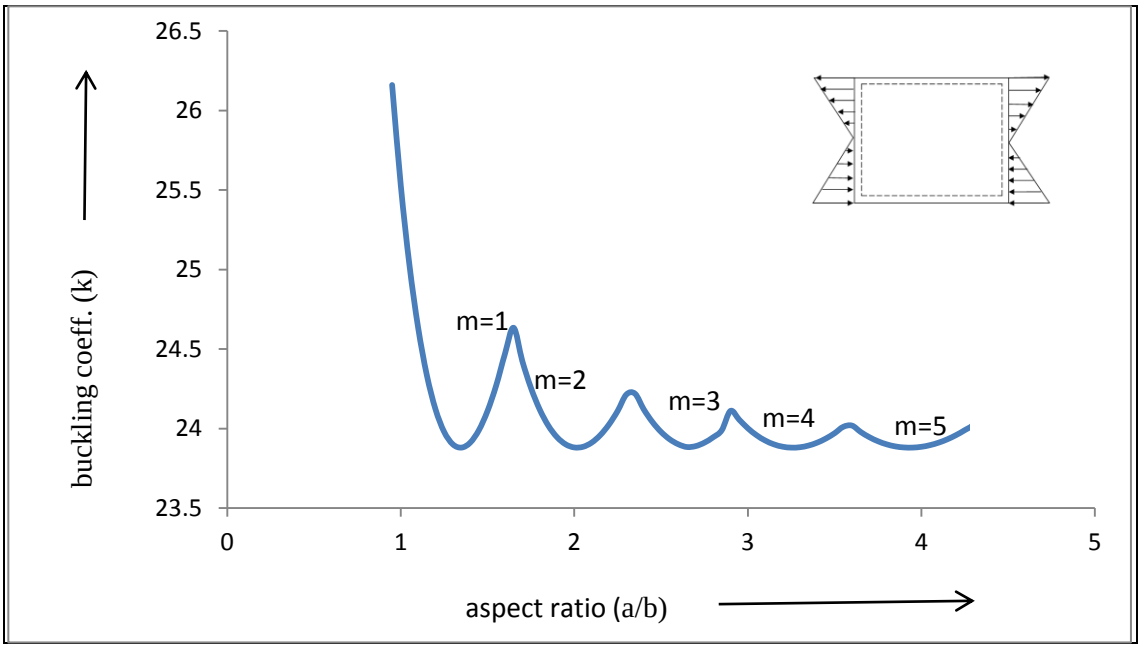

Fig.5 Variation of buckling coefficients of SSSS plate with the aspect ratio (a/b)

In the Fig.5 shows that if we increase the aspect ratio (0 to 5) of the plate , different modes are found. In point where aspect ratio is (a/b=1.65) ,the mode of the plate are changed from m=1 to m=2.similarly the aspect ratio (a/b =2.35,2.90 & 3.60) points are changed the different modes. Also on this loading we seen that the more number of modes are obtained, means the variation in loading from the one end to other end of the plate gives more effect in buckling. In this case the value of the buckling coefficient is also vary high,means high buckling load is prominent.

4.1.1 Buckling Modes of the Simply Supported Rectangular Plates Uniformly Compressed in One Direction:

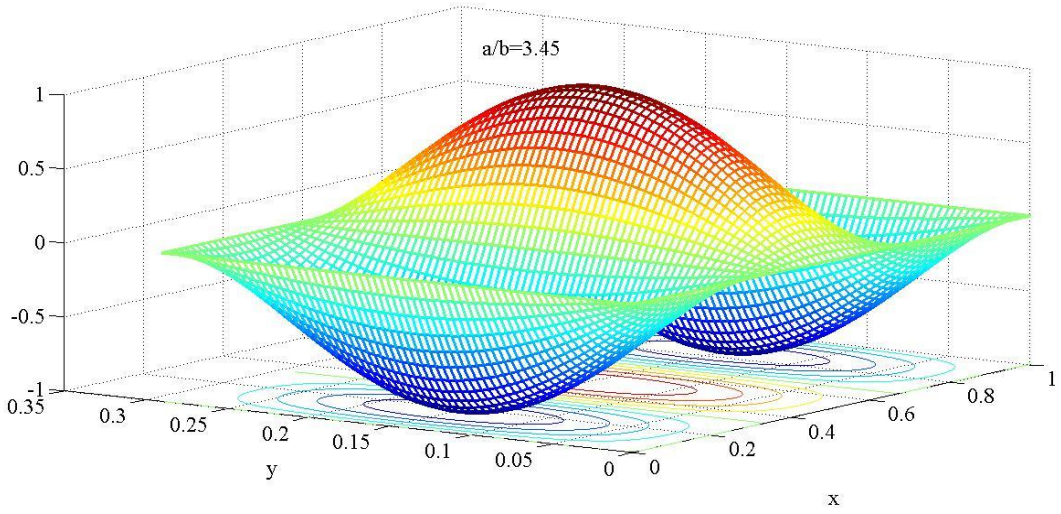

Fig6. Buckling modes for SSSS rectangular isotropic plate under uniform inplane load distributions for aspect ratio (a/b=3.45).

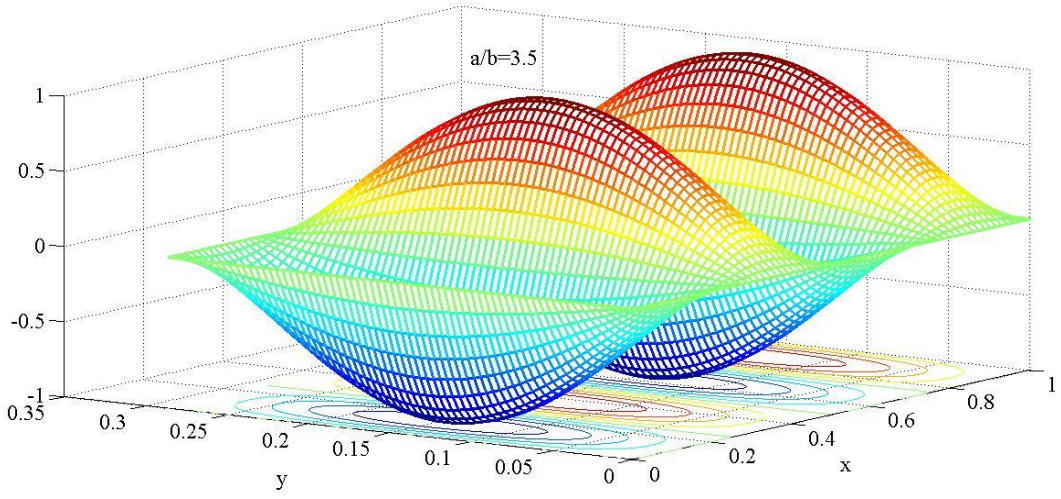

Fig7. Buckling modes for SSSS rectangular isotropic plate under uniform inplane load distributions for aspect ratio (a/b=3.5).

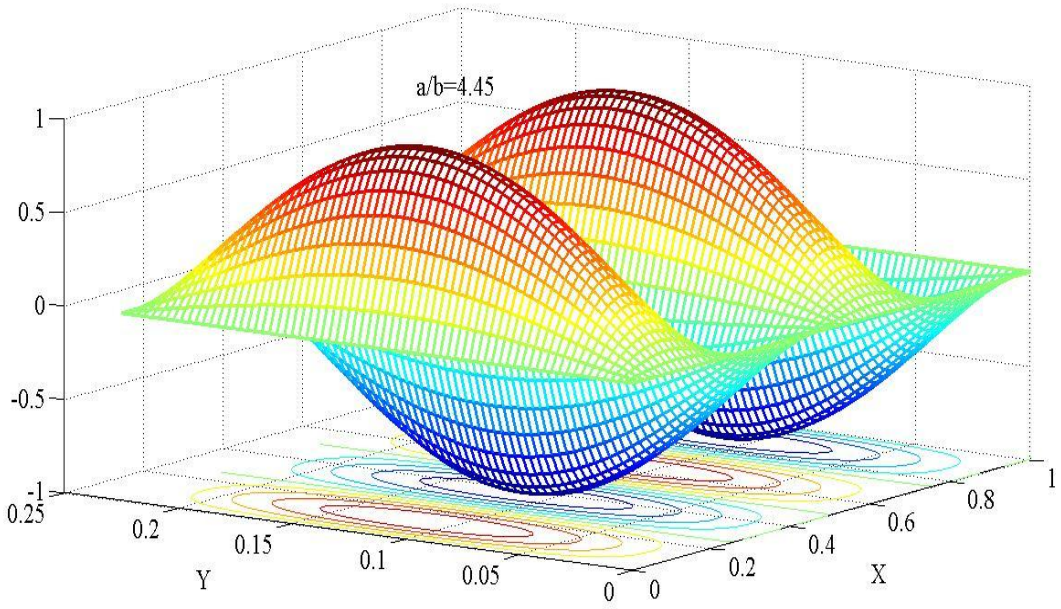

Fig8. Buckling modes for SSSS rectangular isotropic plate under uniform inplane load distributions for aspect ratio (a/b=4.45).

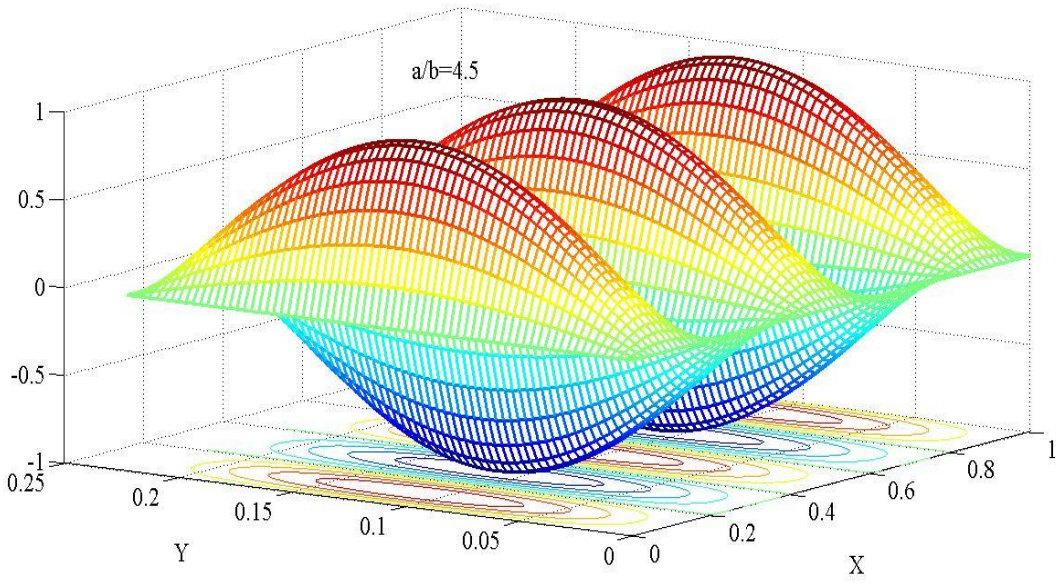

Fig9. Buckling modes for SSSS rectangular isotropic plate under uniform inplane load distributions for aspect ratio (a/b=4.5).

In the Fig.6 the buckle mode for the SSSS rectangular isotropic plate under uniform inplane load distributions (α=0) for aspect ratio (a/b=3.45) is shown. In given aspect ratio (a/b=3.45) the plate is buckle in a 3^{rd} mode. similarly we see the Fig.7 for the aspect ratio (a/b=3.5) for same boundary condition & loading condition are buckle in a 4^{th} mode. So it is clear that the plate is change his mode from m=3 to m=4 between the aspect ratio 3.45 & 3.5.

Similarly we see in Fig.8 the plate is buckle in a 4^{th} mode with aspect ratio (a/b=4.45) and in Fig.9 the plate is buckle in a 5^{th} mode with aspect ratio (a/b=4.5) means that the plate is change his mode from m=4 to m=5 between aspect ratio 4.45 to 4.5.

When the loaded edges are simply supported and applied in-plane load is uniform distributed , the plate buckles in a particular mode along the loading direction depending on length to width ratio of plate and in a combination of two or more modes along unloaded edges.

4.2 Buckling of rectangular plate with different boundary condition applied with uniformly compression:

4.2.1 CSCS Rectangular Plates:

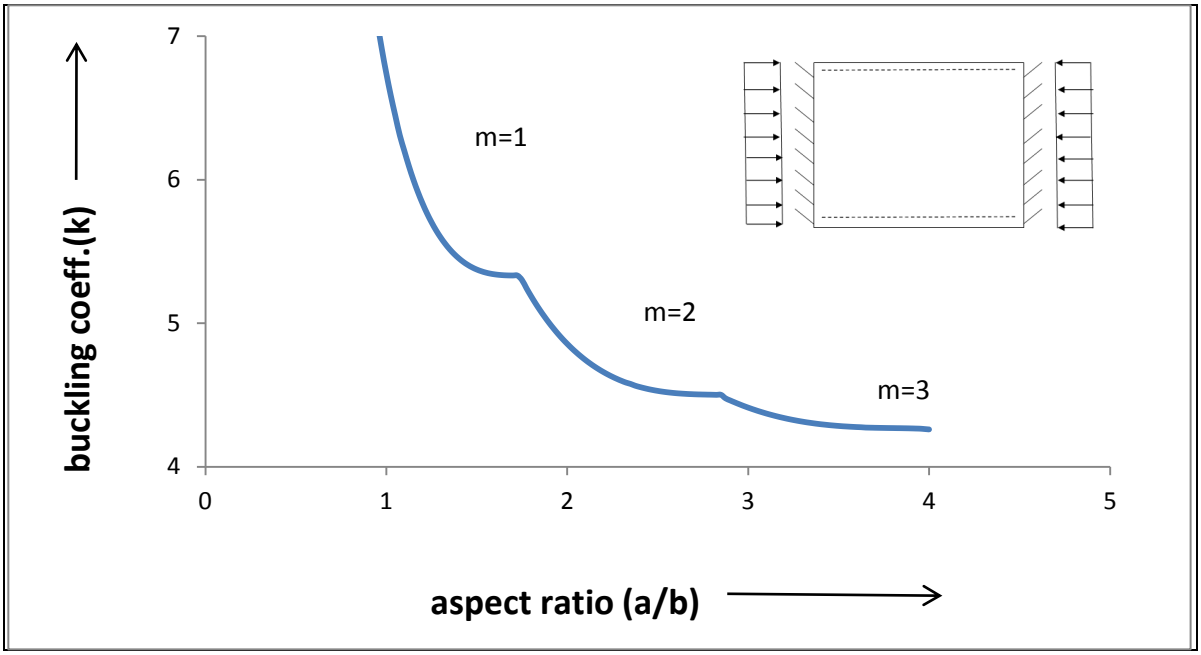

Fig.10 Variation of buckling coefficients of CSCS plate with the aspect ratio (a/b)

The variation of dimensionless buckling load coefficients of a isotropic plate with mixed support condition (CSCS) subjected to linearly varying load against aspect ratio(a/b) of the plate is shown in figure. In the graph shows that if we increase the aspect ratio (0 to 5) of the plate , different modes are found. In point where aspect ratio is (a/b=1.725) ,the mode of the plate are changed from m=1 to m=2.but the point is very sharp, the difference between buckling coefficient is very small because the loading side of the plate is clamped. It is observed from the figure that for very long (a/b>4) plates, the buckling loads is going down.

4.2.2 SCSC Rectangular Plates:

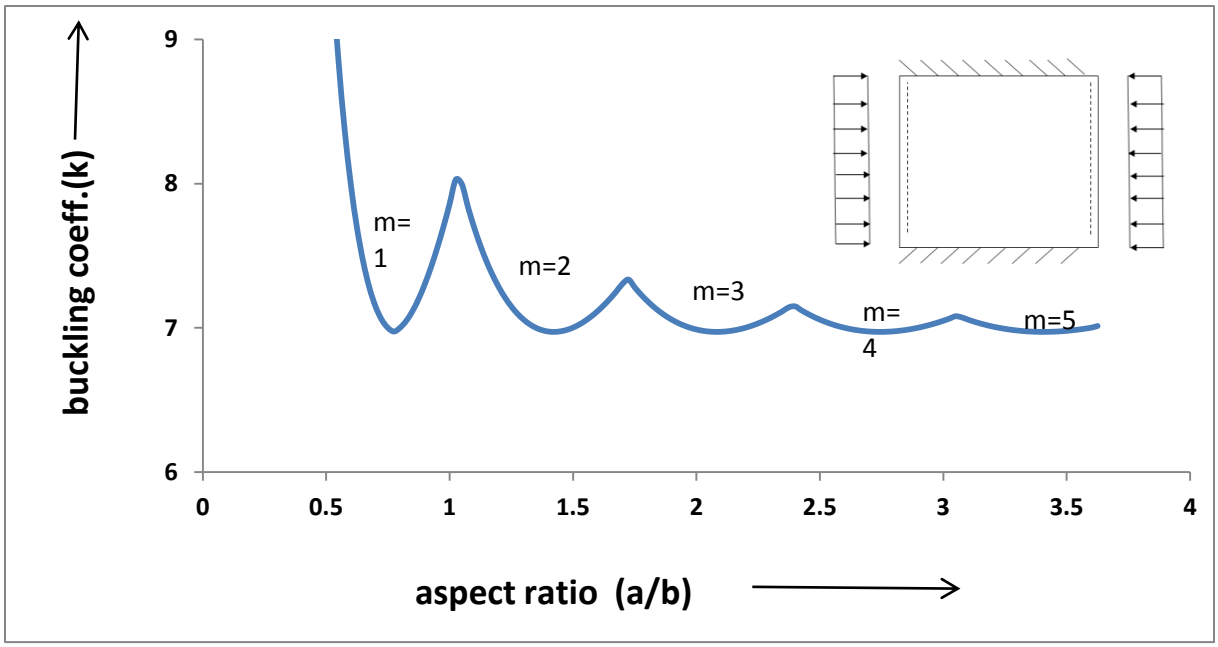

Fig.11 Variation of buckling coefficients of SCSC plate with the aspect ratio (a/b)

The variation of dimensionless buckling load coefficients of a isotropic plate with mixed support condition (SCSC) subjected to linearly varying load against aspect ratio(a/b) of the plate is shown in figure. In the graph shows that if we increase the aspect ratio (0 to 5) of the plate , different modes are found. In point where aspect ratio is (a/b=1.025) ,the mode of the plate are changed from m=1 to m=2 and the point is very clearly shown, the difference between buckling coefficient is uniform because the loading side of the plate is simply supported. It is observed from the figure that for very long (a/b>4) plates, the buckling loads is remains same.

4.2.3 SCSS Rectangular Plates:

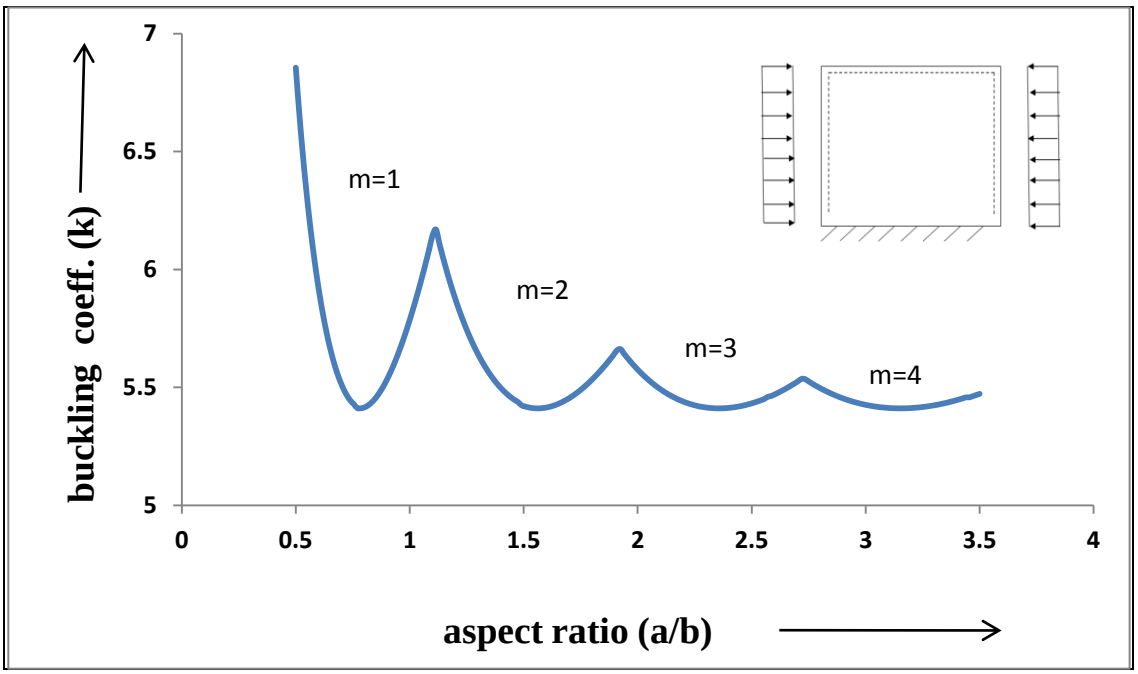

Fig.12 Variation of buckling coefficients of SCSS plate with the aspect ratio (a/b)

The variation of dimensionless buckling load coefficients of a isotropic plate with mixed support condition (SCSS) subjected to linearly varying load against aspect ratio(a/b) of the plate is shown in figure. In the graph shows that if we increase the aspect ratio (0 to 5) of the plate , different modes are found. In point where aspect ratio is (a/b=1.115) ,the mode of the plate are changed from m=1 to m=2.similarly the aspect ratio (a/b =1.945,2.735) points are changed the different modes.The difference between buckling coefficient is uniform because the loading side of the plate is simply supported. It is observed from the figure that for very long (a/b>4) plates, the buckling loads is remains same.

4.2.4 SSCC Rectangular Plates Uniformly :

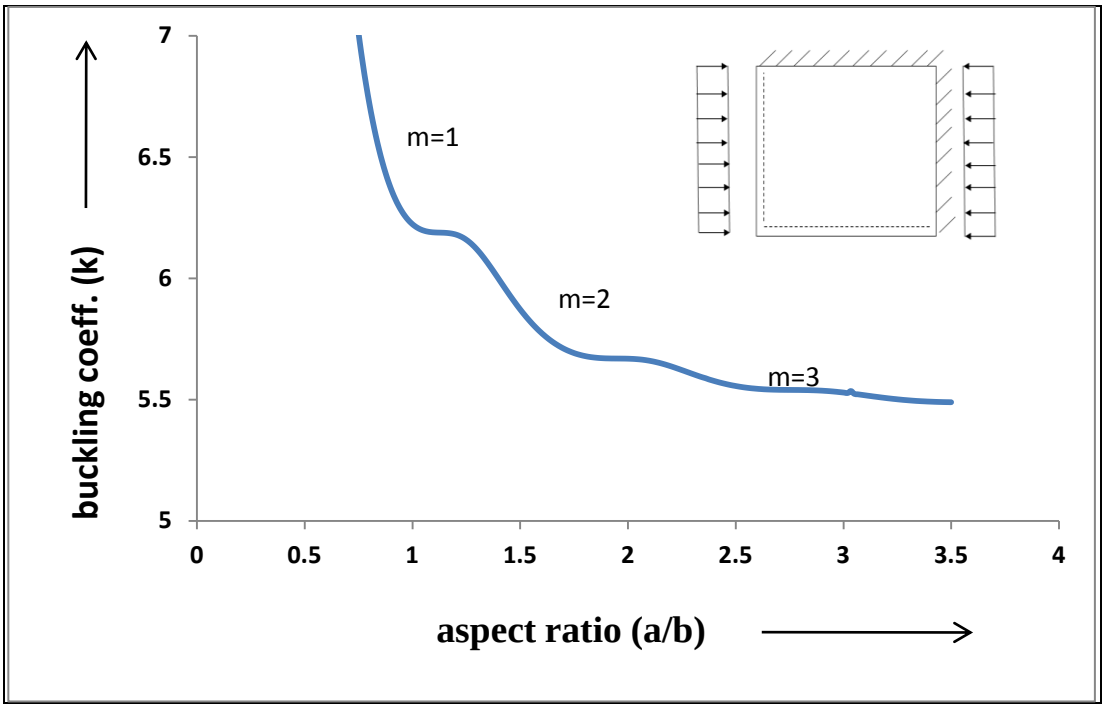

Fig.13 Variation of buckling coefficients of SSCC plate with the aspect ratio (a/b)

The variation of dimensionless buckling load coefficients of a isotropic plate with mixed support condition (SSCC) subjected to linearly varying load against aspect ratio(a/b) of the plate is shown in figure. In the graph shows that if we increase the aspect ratio (0 to 5) of the plate , different modes are found. In point where aspect ratio is (a/b=1.145) ,the mode of the plate are changed from m=1 to m=2.but the point is very sharp, and but the in point the constant value of buckling coefficient are found the difference between buckling coefficient is very small because the one end of loading side of the plate is simply supported and one end is clamped. It is observed from the figure that for very long (a/b>4) plates, the buckling loads is going down.

4.2.5 SSCS Rectangular Plates:

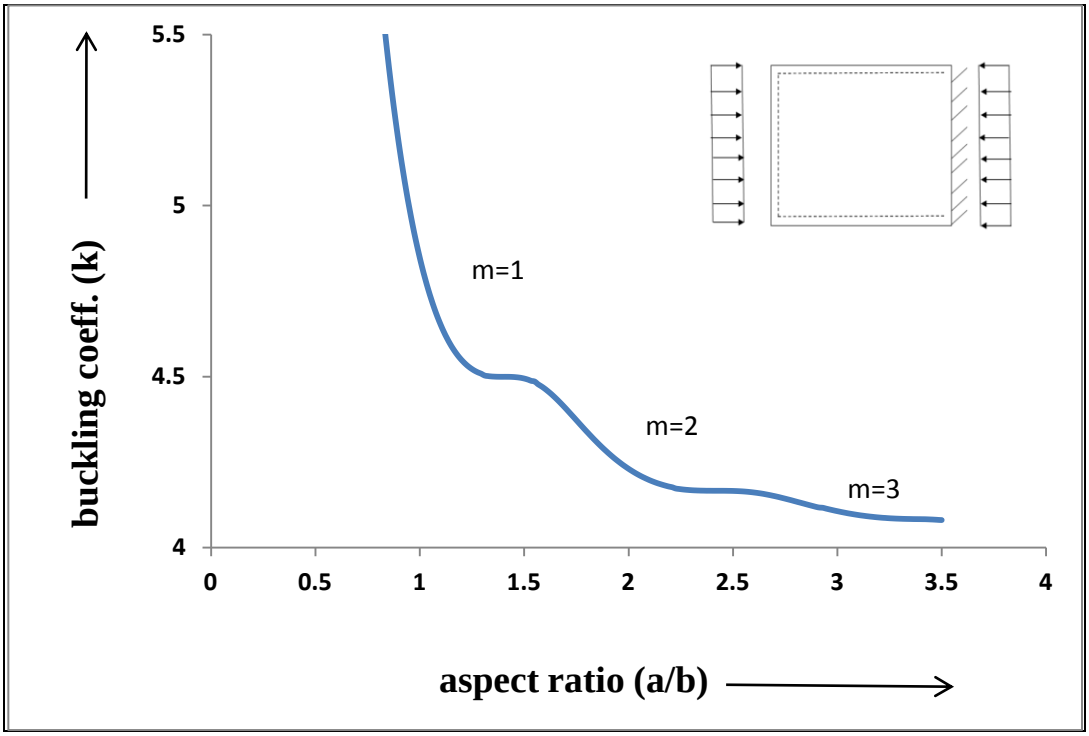

Fig.14 Variation of buckling coefficients of SSCS plate with the aspect ratio (a/b)

The variation of dimensionless buckling load coefficients of a isotropic plate with mixed support condition (SSCS) subjected to linearly varying load against aspect ratio(a/b) of the plate is shown in figure. In the graph shows that if we increase the aspect ratio (0 to 5) of the plate , different modes are found. In point where aspect ratio is (a/b=1.385) ,the mode of the plate are changed from m=1 to m=2.but the in point the constant value of buckling coefficient are found and the difference between buckling coefficient is very small because the one end of loading side of the plate is simply supported and one end is clamped. It is observed from the figure that for very long (a/b>4) plates, the buckling loads is going down.

4.2.6 CCCC Rectangular Plates:

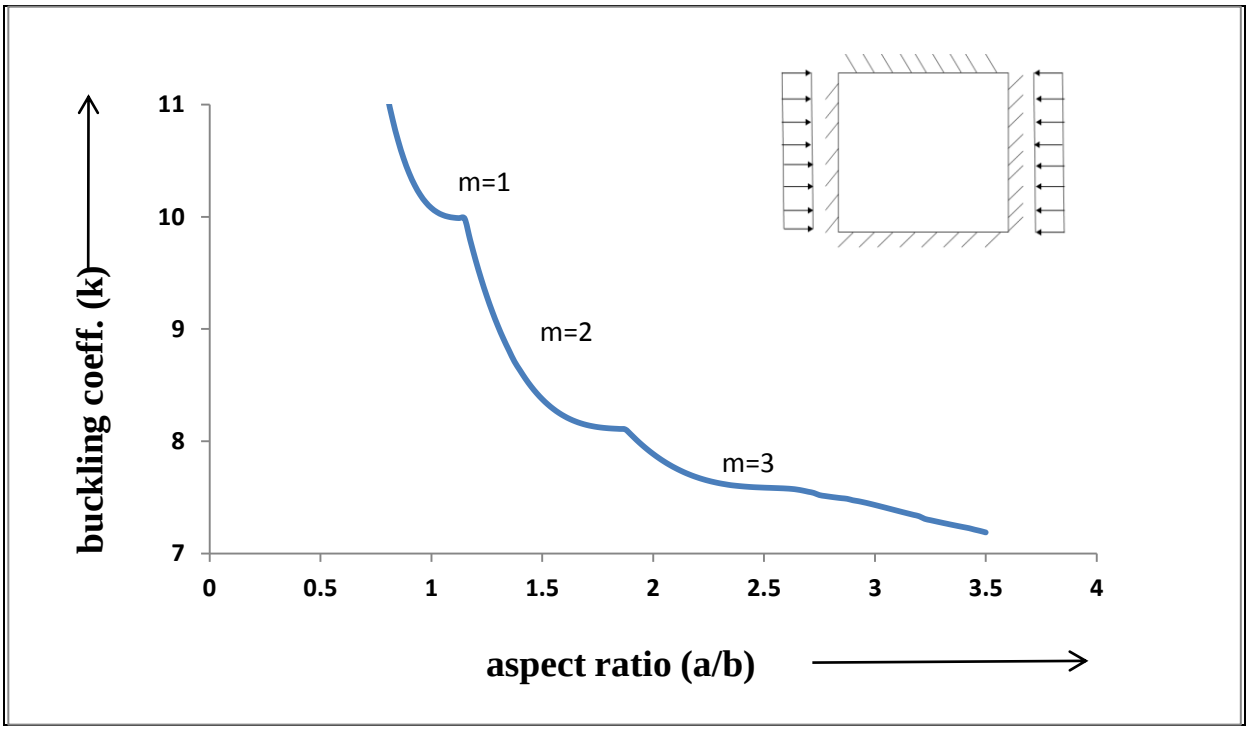

Fig.15 Variation of buckling coefficients of CCCC plate with the aspect ratio (a/b)

The variation of dimensionless buckling load coefficients of a isotropic plate with mixed support condition (CCCC) subjected to linearly varying load against aspect ratio(a/b) of the plate is shown in figure. In the graph shows that if we increase the aspect ratio (0 to 5) of the plate , different modes are found. In point where aspect ratio is (a/b=1.15) ,the mode of the plate are changed from m=1 to m=2.but the in point the constant value of buckling coefficient are found and the difference between buckling coefficient is very small because the both end of loading side of the plate is clamped. It is observed from the figure that for very long (a/b>3.5) plates, the buckling loads is going down.

4.2.6 CCCS Rectangular Plates:

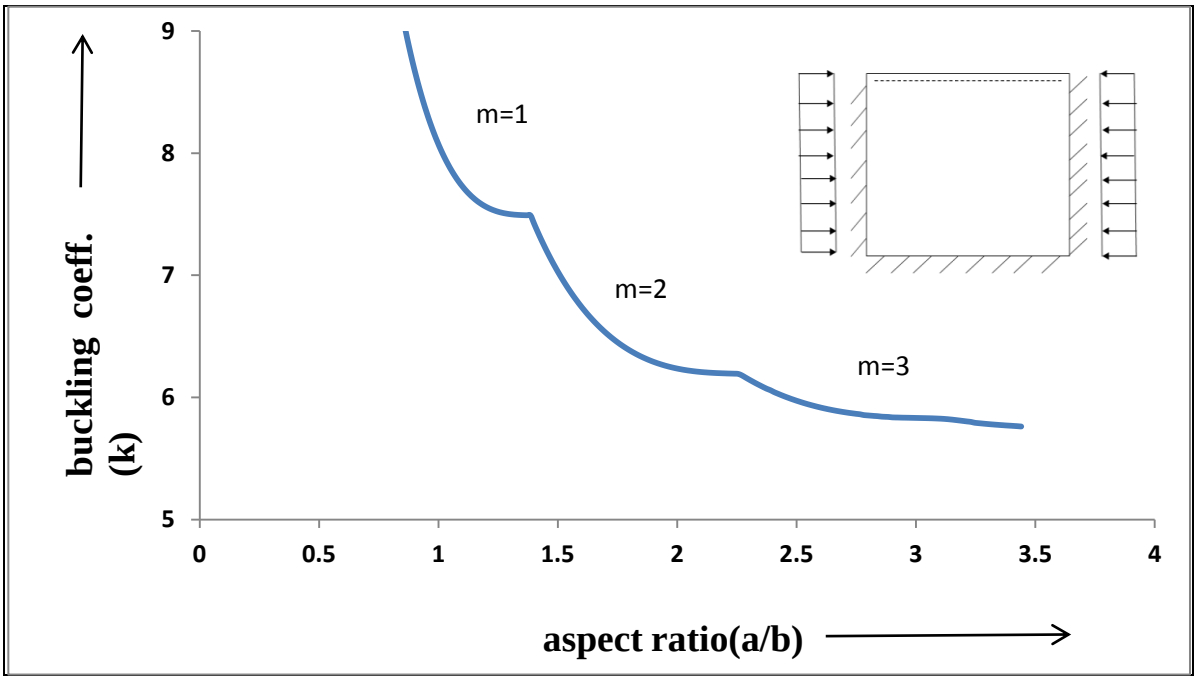

Fig.16 Variation of buckling coefficients of CCCS plate with the aspect ratio (a/b)

The variation of dimensionless buckling load coefficients of a isotropic plate with mixed support condition (CCCS) subjected to linearly varying load against aspect ratio(a/b) of the plate is shown in figure. In the graph shows that if we increase the aspect ratio (0 to 5) of the plate , different modes are found. In point where aspect ratio is (a/b=1.385) ,the mode of the plate are changed from m=1 to m=2.but the in point the constant value of buckling coefficient are found and the difference between buckling coefficient is very small because the both end of loading side of the plate is clamped. It is observed from the figure that for very long (a/b>3.5) plates, the buckling loads is going down.

4.2.8 CCSC Rectangular Plates:

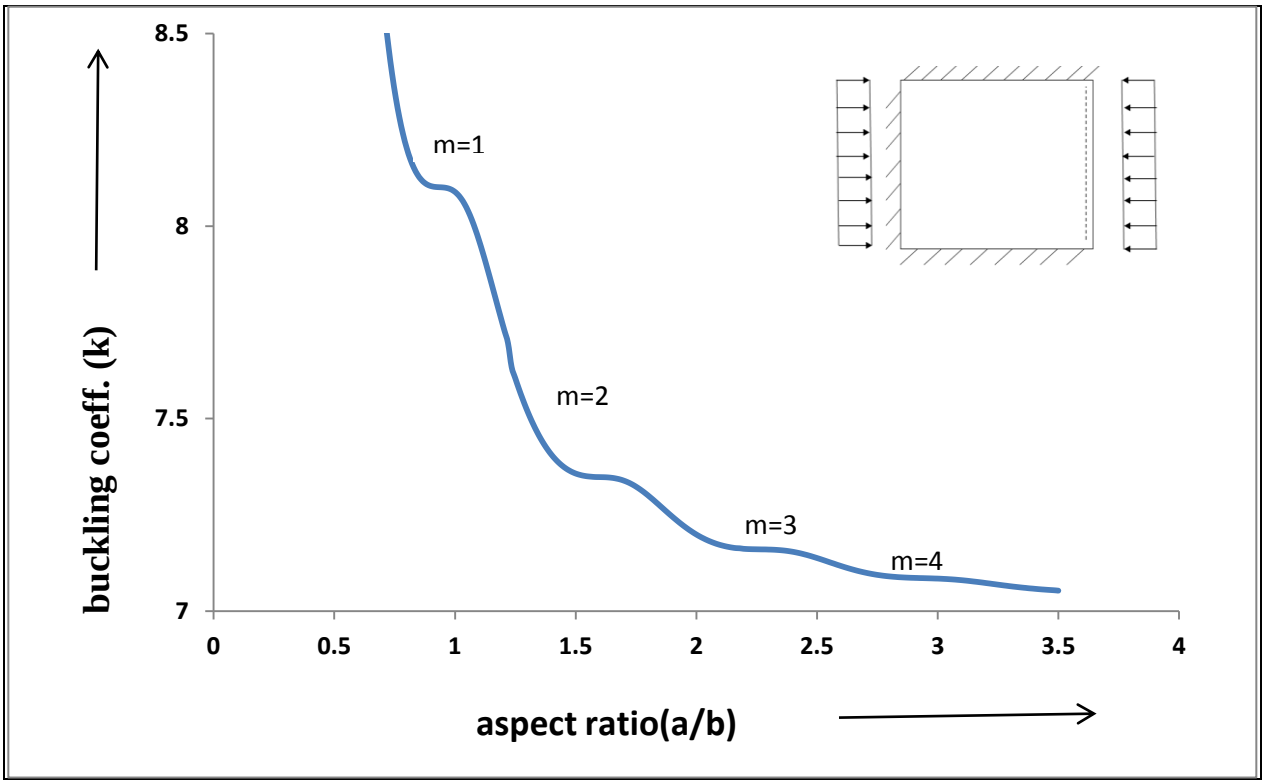

Fig.17 Variation of buckling coefficients of CCSC plate with the aspect ratio (a/b)

The variation of dimensionless buckling load coefficients of a isotropic plate with mixed support condition (CCSC) subjected to linearly varying load against aspect ratio(a/b) of the plate is shown in figure. In the graph shows that if we increase the aspect ratio (0 to 5) of the plate , different modes are found. In point where aspect ratio is (a/b=1.385) , the constant value of buckling coefficient are found and the difference between buckling coefficient is very small because the one end of loading side of the plate is clamped and other side is simply supported the remain other to side is clamped. It is observed from the figure that for very long (a/b>3.5) plates, the buckling loads is going down.

5. Conclusion:

In the present problem the stress distributions with in the plate is same as the applied in-plane stresses in the plate edge . Using this stress distribution and adopting Galerkin's approximation the critical buckling loads are evaluated. Beam functions are used as shape functions in the Galerkin's technique. It is observed that, whenever the plate restrained condition increases, the number of terms required is more to get the converged buckling load. When the two loaded edges are simply supported and applied in plane load is uniform or linearly varying, the plate buckles with a particular number of half-waves in the loading direction depending on the length to width ratio of the plate and incombination of two or more half-waves along the unloaded edge. If the applied inplane loading is non-uniform the buckling mode is combination of two or more half-waves in both loaded direction as well as the unloaded direction independent of boundary conditions. As the applied load is pure bending type we need to take six terms in x-direction and six terms in y-direction to get the converged buckling load for maximum restrained plate i.e. CCCC plate. For other boundary conditions less number of terms is required to get the converged solution. It is observed that for the same aspect ratio, the SCSS and SCSC boundary condition plate buckles into more number of half-waves due to the increase in boundary restraint.

6. References

[1] **Leissa AW, Kang JH**. Exact solution for vibration and buckling of an SS–C– SS–C rectangular plate loaded by linearly varying inplane stresses. *International Journal of Mechanical Science 2002;44:1925–9455.*

[2] **Sarat Kumar Panda, L.S. Ramachandra** , Buckling of rectangular plates with various boundary conditions loaded by non-uniform inplane loads *"International Journal of Mechanical Sciences" 52 (2010) 819–828.*

[3] **Sarat Kumar Panda and L. S. Ramachandra.**Buckling and Postbuckling Behavior of Cross-Ply Composite Plate Subjected to Nonuniform In-Plane Loads."*American Society for Civil Engineers*" *137(9), 589-597.*

[4] **Kang JH, Leissa AW**. buckling of SS–F–SS–F rectangular plates loaded by in-plane moments. "*International Journal of Structural Stability and Dynamics 2001;1(4):527–43"*.

[5] **Kang JH, Leissa AW**. Exact solution for the buckling of rectangular plates having linearly varying in-plane loading on two opposite simply supported edges . "*International Journal of Mechanical Science 2005;42:4220–38."*

[6]**L.S. Ramachandra and Sarat Kumar Panda.,** 2011. Dynamic instability of composite plates subjected to non-uniform in-planeloads, *Journal of Sound and Vibration, 331, 53-65.*

[7] **Timoshenko, S.P. and Gere, J.M.,** 1961. *Theory of elastic stability*,McGraw-Hill, New delhi.

[8] **Timoshenko and Krieger.,** 1959. *Theory of plates and shells* , McGraw-Hill, New delhi